Tetherin antagonism by the Ebola virus glycoprotein requires an intact receptor-binding domain and can be blocked by GP1-specific antibodies

Constantin Brinkmann,[a] Inga Nehlmeier,[a] Kerstin Walendy-Gnirß,[a] Julia Nehls,[b,c] Mariana González Hernández,[a] Markus Hoffmann,[a] Xiangguo Qiu,[d] Ayato Takada,[e] Michael Schindler,[b,c] and Stefan Pöhlmann[a,*]

Infection Biology Unit, German Primate Center, Göttingen, Germany[a]; Molecular Virology of Human Infectious Diseases, University Hospital Tübingen, Institute of Medical Virology and Epidemiology, Tübingen, Germany[b]; Institute of Virology, Helmholtz Zentrum München, German Research Center for Environmental Health, Neuherberg, Germany[c]; Special Pathogens Program, National Microbiology Laboratory, Public Health Agency of Canada, Winnipeg, Canada[d]; Division of Global Epidemiology, Hokkaido University Research Center for Zoonosis Control, Sapporo, Japan[e].

Current address KWG: Viral Zoonosis and Adaptation Research Group, Heinrich-Pette-Institute, Hamburg, Germany

*Corresponding author. Please direct correspondence to: Infection Biology Unit, Deutsches Primatenzentrum, Kellnerweg 4, 37077 Göttingen, Germany. Phone: +49 551 3851 150, Fax: +49 551 3851 184, E-mail: spoehlmann@dpz.eu

Running title: Tetherin antagonism by Ebola virus

ABSTRACT

The glycoprotein of Ebola virus (EBOV-GP), a member of the *Filoviridae* family, facilitates viral entry into target cells. In addition, EBOV-GP antagonizes the antiviral activity of the host cell protein tetherin, which may otherwise restrict EBOV-release from infected cells. However, it is unclear how EBOV-GP antagonizes tetherin and it is unknown whether the GP of Lloviu virus (LLOV), a filovirus found in dead bats in Northern Spain, also counteracts tetherin. Here, we show that LLOV-GP antagonizes tetherin, indicating that tetherin may not impede LLOV spread in human cells. Moreover, we demonstrate that appropriate processing of N-glycans in tetherin/GP-coexpressing cells is required for tetherin counteraction by EBOV-GP. Furthermore, we show that an intact receptor-binding domain (RBD) in the GP1 subunit of EBOV-GP is a prerequisite to tetherin counteraction. In contrast, blockade of Niemann-Pick disease, type C1 (NPC1), a cellular binding partner of the RBD, did not interfere with tetherin antagonism. Finally, we provide evidence that an antibody directed against GP1, which protects mice from a lethal EBOV challenge, may block GP-dependent tetherin antagonism. Our data in conjunction with previous reports indicate that tetherin antagonism is conserved between the GPs of all known filoviruses and demonstrate that the GP1 subunits of EBOV-GP plays a central role in tetherin antagonism.

IMPORTANCE

Filoviruses are re-emerging pathogens that constitute a public health threat. Understanding how Ebola virus (EBOV), a highly pathogenic filovirus responsible for the 2013-2016 Ebola virus disease epidemic in Western Africa, counteracts antiviral effectors of the innate immune system might help to define novel targets for antiviral intervention. Similarly, determining whether Lloviu virus (LLOV), a filovirus detected in bats in Northern Spain, is inhibited by innate antiviral effectors in human cells might help to define whether the virus constitutes a threat to humans. The present study shows that LLOV like EBOV counteracts the antiviral effector protein tetherin via its glycoprotein (GP), suggesting that tetherin does not pose a defense against LLOV spread in humans. Moreover, our work identifies the GP1 subunit of EBOV-GP, in particular an intact receptor-binding domain, as critical for tetherin counteraction and provides evidence that antibodies directed against GP1 can interfere with tetherin counteraction.

INTRODUCTION

The infection with Ebola virus (EBOV, formerly Zaire ebolavirus), a member of the genus *Ebolavirus* within the family *Filoviridae*, causes severe and frequently fatal disease. The Ebola virus disease (EVD) epidemic in Western Africa in 2013-2016 was associated with 11,316 deaths and entailed secondary cases in the US and Spain (1, 2), indicating that EVD constitutes a global public health threat. The interferon (IFN) system, an important component of innate immunity, constitutes a first line defense against infection by EBOV and other viruses (3, 4). Sensors of the IFN system detect viral invaders and trigger the production and release of IFN. Binding of IFN to receptors on neighboring cells in turn induces the expression of roughly 300-400 proteins, many of which exert antiviral activity (5). As a consequence, IFN exposed cells transit into an antiviral state. Understanding how IFN-induced antiviral factors reduce EBOV infection and how the virus evades this process might yield insights into viral pathogenesis and might help to establish targets for intervention.

The IFN-induced antiviral factor tetherin (CD317, BST-2, HM1.24) restricts release of progeny virions form infected cells (6, 7). Tetherin's particular membrane topology is pivotal to this activity: The protein has an N-terminal transmembrane domain and a C-terminal glycosylphosphatidylinositol (GPI) anchor, which permit tetherin to simultaneously insert into the viral and the plasma membrane. As a consequence, tetherin forms a physical tether between newly formed virus particles and the host cell (8). Several viruses encode tetherin antagonist which allow for robust viral spread in tetherin-positive target cells (9). The Vpu protein of HIV-1 is the prototype tetherin antagonist and it is well established that specific interactions between the transmembrane domains of these proteins are required for tetherin antagonism (10-13). Antagonism encompasses Vpu-dependent removal of tetherin from the site of viral budding, the plasma membrane, and re-routing of the protein for endosomal degradation (14-16).

97 The glycoprotein (GP) of filoviruses is inserted into the viral envelope and facilitates viral
98 entry into target cells, a process that depends on the interactions of the receptor binding domain
99 (RBD) in GP with the cellular protein Niemann-Pick disease, type C1 (NPC1) (17, 18).
100 Moreover, EBOV-GP counteracts tetherin (19) by a novel mechanism (19-22), which might
101 involve GP-dependent inhibition of tetherin association with the viral matrix protein, VP40 (23).
102 Tetherin antagonism by GP might be required for efficient EBOV spread in the host, since
103 macrophages, central viral target cells (24), express tetherin (25, 26). In contrast, it is unknown
104 whether the GP of a related filovirus, Lloviu virus (LLOV, genus *Cuevavirus*) (27), counteracts
105 tetherin. In addition, it is poorly understood which domains in EBOV- GP contribute to tetherin
106 counteraction. EBOV-GP was found to interact with tetherin via its transmembrane unit, GP2
107 (20), and evidence was provided that the transmembrane domain (TM) within GP2 is necessary
108 but not sufficient for tetherin counteraction (28, 29). However, the EBOV-GP TM mutant unable
109 to counteract tetherin was also defective in mediating viral entry (28) and might thus have been
110 partially misfolded. In addition, a separate study revealed that EBOV-GP counteracts an artificial
111 tetherin molecule (21), suggesting that GP binding to tetherin may not be required for
112 antagonism. More recent work indicated that deletion of the glycan cap of EBOV-GP, a N-
113 glycosylated region displayed at the top of GP, might be incompatible with tetherin antagonism
114 (29) but the underlying mechanism was not investigated. In sum, it is at present unknown how
115 EBOV-GP antagonizes tetherin and it is incompletely understood which determinants in the viral
116 GP control tetherin antagonism.
117 Here, we analyzed whether LLOV-GP antagonizes tetherin and we examined the role of
118 the surface unit, GP1, of EBOV-GP in tetherin antagonism. We show that LLOV-GP counteracts
119 the antiviral activity of tetherin, indicating that tetherin might not pose an effective barrier against
120 LLOV spread in human cells. Moreover, we demonstrate that appropriate processing of N-

glycans as well as an intact RBD are required for tetherin counteraction by EBOV-GP although inhibition of the RBD interaction partner NPC1 has no effect. Finally, we identified an antibody directed against the GP1 subunit of EBOV-GP that may block tetherin antagonism. These results indicate a central role of the GP1 subunit of EBOV-GP in tetherin counteraction and suggest that antibodies directed against this subunit can interfere with viral release by blocking GP-dependent tetherin antagonism.

145 **MATERIAL AND METHODS**

146

147 **Cell culture, plasmids and antibodies.** Human embryonal kidney 293T cells, N-acetyl
148 glucosamine transferase I (GnTI) deficient HEK293S GnTI$^-$ cells (30) and HeLa cells were
149 maintained in Dulbecco's Modified Eagle Medium (DMEM, Invitrogen) supplemented with 10%
150 fetal bovine serum (FBS), 1% penicillin/streptomycin and, in case of GnTI$^-$ cells, 10 µM sodium
151 pyruvate. Mouse hybridoma cells secreting anti-VSV-G antibody (I1-hybridoma, CRL-2700,
152 ATCC) were cultivated in cultivated in DMEM, supplemented with 20% FBS and 1%
153 penicillin/streptomycin. Cells were cultured at 37°C in humidified atmosphere containing 5%
154 CO_2. Plasmids encoding the following proteins were described previously: Tetherin (31), EBOV-
155 GP wt and EBOV-GP with mutations in the RBD (32), deleted mucin-like domain (MLD) (33) or
156 inactivated furin cleavage site (34), LLOV-GP (35), HIV Vpu (20), vesicular stomatitis virus
157 glycoprotein (VSV-G, (36)), murine leukemia virus (MLV) vector encoding luciferase (36),
158 MLV Gag-Pol (36), HIV-1 p55-Gag (28) and EBOV-VP40 harboring a myc tag (37). Tetherin
159 with an N-terminal AU1 antigenic tag was generated by PCR-based mutagenesis and inserted
160 into plasmid pcDNA3.1 using EcoRV and NheI restriction sites. The integrity of the PCR
161 amplified sequence was confirmed by automated sequence analysis. The following antibodies
162 have also been previously described: EBOV-GP1 specific monoclonal antibodies (38, 39), anti-
163 Gag monoclonal antibody (40) and a polyclonal rabbit antiserum raised against EBOV-GP1 (41).
164 The following antibodies were purchased from commercial providers: monoclonal anti-V5-
165 antibody (Invitrogen);); mouse anti-AU1-antibody (Covance); monoclonal rabbit anti-tetherin
166 antibody(Abcam); anti-tetherin monoclonal antibody (B02P, Abnova); polyclonal anti-ß-actin
167 antibody (Abnova, Sigma) and horseradish-peroxidase (HRP)-coupled secondary antibodies

168 directed against mouse and rabbit immunoglobulin (Dianova) and FITC-coupled secondary
169 antibodies against mouse immunoglobulin (Dianova).
170
171 **Analysis of viral glycoprotein-mediated transduction.** Transduction has been analyzed as
172 described (36). In brief, for the production of MLV-vectors bearing filovirus GPs, 293T control
173 or GnTI$^-$ cells were seeded in T25 cell culture flasks and cotransfected with plasmids encoding
174 MLV Gag-Pol, an MLV vector encoding firefly luciferase and a viral glycoprotein or empty
175 plasmid, employing calcium phosphate as transfection reagent. At 16 h post transfection the cells
176 were washed and supplemented with fresh medium. At 48 h post transfection the culture
177 supernatants were collected, sterile filtered through a 0,45 µm filter, aliquoted and stored at -
178 80°C. For transduction of target cells, 293T cells seeded in a 96 well plate were incubated with
179 50 µl/well of vector preparation for 6 h at 37°C. Thereafter, 50 µl/well of fresh DMEM culture
180 medium was added. At 72 h post transduction, the culture supernatants were removed and cells
181 were lysed and luciferase activity measured in cell lysates employing a commercially available
182 kit (PJK) and the Hidex CHAMELEON V luminometer with Microwin 2000 software.
183 For analysis of the antiviral activity of U18666A and cationic amphiphiles, VSV-based
184 pseudotypes were used for consistency with previous work (42). Pseudotypes were generated and
185 used for transduction as described (43). In brief, 293T cells seeded in 6 well-plates were calcium
186 phosphate transfected with plasmids encoding VSV-G or EBOV-GP or empty plasmid
187 (pCAGGS) as negative control. At 18 h post transfection, the cells were inoculated with
188 VSV*ΔG-Luc (44, 45) at an MOI of 3 for 1 h at 37°C. Thereafter, the cells were washed with
189 PBS and incubated for 1 h at 37°C with a 1:1,000 dilution of hybridoma supernatant containing
190 anti-VSV-G antibody in order to neutralize residual virus. Finally, fresh culture medium was
191 added to the cells and supernatants were collected at 18-20 h post transduction, clarified from cell

192 debris by centrifugation, aliquoted and stored at -80°C. To assess blockade of viral entry by
193 cationic amphiphiles, 293T target cells seeded in 96-well plates were pre-incubated with each
194 compound or diluent for 3 h at 37°C. Subsequently, the cells were inoculated with equal volumes
195 of pseudotypes and incubated for 18 h at 37°C in the presence of inhibitor. Finally, luciferase
196 activities in cell lysates were measured as described for cells transduced with MLV-pseudotypes.
197
198 **Inhibition of virus-like particle release by tetherin and tetherin antagonism by filoviral**
199 **glycoproteins.** Release of virus-like particles (VLPs) and its inhibition by tetherin has been
200 examined as described (20, 28). In brief, 293T control cells or GnTI$^-$ cells were seeded in 48 well
201 plates and cotransfected with plasmids encoding HIV-1 p55-Gag, tetherin and a potential tetherin
202 antagonist or empty plasmid, using the calcium phosphate method. For experiments with EBOV-
203 VP40, a plasmid encoding VP40 instead of HIV-Gag was used. At 16 h post transfection, the
204 transfection medium was replaced by fresh culture medium. For blockade of EBOV-GP-
205 dependent tetherin antagonism, GP1-specific monoclonal antibodies were added to the culture
206 medium at a final concentration of 20 µg/ml or cationic amphiphiles (U18666A, Clomifene,
207 Terconazole; all purchased from Sigma) were added at the indicated concentrations. At 48 h post
208 transfection the supernatants were collected and the cells were lysed in 50 µl of 2x SDS-
209 containing lysis buffer (30 mM Tris [pH 6.8], 10% glycerol, 2% SDS, 5% β-mercaptoethanol,
210 0.1% bromphenol blue, 1mM EDTA). The lysates were incubated at 95°C for 30 min. The
211 supernatants were cleared of remaining cell debris by centrifugation and VLPs were pelleted
212 from cleared supernatants by centrifugation through a 20% sucrose cushion. The concentrated
213 VLPs were lysed in 30 µl 2 x SDS loading buffer and incubated at 95°C for 30 min.
214 Subsequently, cell lysates and lysed supernatants were investigated for the presence of Gag or
215 VP40, respectively, employing Western blot analysis.

Immunoblotting. For immunoblotting, the proteins were separated via SDS-polyacrylamid gel electrophoresis using a 12.5% polyacrylamide gel and transferred onto a nitrocellulose membrane (GE Lifesciences, 0.2 µm). The membranes were blocked in 5% milk powder in PBS with 0,1% Tween 20 and Gag-protein was detected using 1:100 diluted supernatants of hybridoma cells secreting a mouse anti-Gag antibody. If murine antibodies against EBOV-GP were added to inhibit tetherin antagonism, Gag expression was detected using a human monoclonal anti-Gag antibody at a dilution of 1:5,000. VP40 was detected using 1:3 diluted supernatants of a hybridoma cell line which secrets anti-myc antibody. Expression of EBOV-GP wt and mutants was detected employing a GP1-specific rabbit serum at a dilution of 1:1,000. For the detection of LLOV-GP, a V5-tagged version of this protein was employed and its expression detected employing an anti-V5 antibody at a dilution of 1:5,000. Expression of ß-actin was detected after stripping the membranes (Tris-HCl, SDS, ß-mercaptoethanol, 50°C, 30 min) employing anti-ß-actin antibodies at a dilution of 1:10,000. HRP-coupled anti-mouse, anti-rabbit and anti-human secondary antibodies were used at a final concentration of 0.1 µg/ml. Bound secondary antibodies were detected using a commercially available ECL kit (GE Healthcare) and signals were visualized using the ChemoCam imaging system and the ChemoStarProfessional software (Intas). For quantification of the signal intensity, the program ImageJ was used (46). For normalization, Gag/VP40 signals measured in culture supernatants were divided by the respective signals detected in cell lysates.

Analysis of Ebola virus glycoprotein expression at the cell surface. For analysis of the surface expression of EBOV-GP and mutants, 293T cells were transfected with the respective plasmids and washed and harvested in PBS at 48 h post transfection. Expression of EBOV-GP at the cell

surface was detected by employing GP-specific mouse monoclonal antibody 5E6 and an FITC-conjugated anti-mouse secondary antibody. Staining of cells fixed with 2% paraformaldehyde was analyzed employing a LSR II Flow Cytometer (BD Biosciences) and the FACS Diva software (BD Biosiences). The data was further analyzed using the FCS Express 4 Flow research software (De Novo software).

Co-immunoprecipitation. For the analysis of EBOV-GP interactions with tetherin by co-immunoprecipitation (CoIP), 293T cells were cotransfected with plasmids encoding EBOV-GP wt or EBOV-GP with mutations in the RBD and a plasmid encoding tetherin with an AU1 antigenic tag added to the N-terminus. In parallel, antibody-agarose conjugates for immunoprecipitation were generated. For this, agarose beads (A/G Plus Agarose, Santa Cruz) were washed two times with CoIP buffer (50 mM Tris/HCl pH8; 150 mM NaCl; 5 mM EDTA; 0,5% IGEPAL), blocked with cold water fish gelatine at 4°C for 2 h on a rotating shaker, washed again with CoIP buffer and incubated with anti-AU1 antibody for 2 h at 4°C on a rotating shaker. At 48 h post transfection, the 293T cells were harvested, washed with PBS and resuspended in CoIP buffer. After lysis for 20 min at 4°C the solutions were cleared from cellular debris by centrifugation at 600 g and aliquoted. Aliquots were stored for subsequent analysis by immunoblotting or were incubated with agarose-bound anti-AU1 antibody for 20 min at room temperature. After washing eight times with Co-IP buffer, the agarose-beads were resuspended in 20 µl of 2x SDS loading dye and analyzed by immunoblotting.

Proximity ligation assay. For analysis of EBOV-GP interactions with tetherin via proximity ligation assay (PLA), 100,000 HeLa cells per well were seeded in 12-well plates containing coverslips and then transfected with the indicated EBOV-GP expression plasmids using

Lipofectamine 2000 according to the manufacturer's protocol (Thermo Fisher). At 24 h post transfection, the cells were fixed for 20 min with 2% PFA at 4°C, permeabilized for 10min with 1% Saponin and blocked for 1 h with 10% FCS at room temperature. The primary antibodies, an anti-tetherin monoclonal antibody (B02P, Abnova) and a rabbit anti-EBOV-GP serum raised against the GP1 subunit (41), were diluted 1:100 and 1:500 in 1% FCS, respectively, and cells were subsequently incubated in the primary antibody solution for 1 h at room temperature. Incubation with PLA probes, ligation reaction, amplification reaction and mounting of the coverslips was performed according to the manufacturer's protocol (Duolink, Sigma Aldrich). Finally, staining was analyzed employing spinning disc microscopy and image analysis as described before (47).

Sequence alignment. The alignment of a portion of the filovirus RBDs was performed using Clustal Omega (http://www.ebi.ac.uk/Tools/msa/clustalo/). Sequences were obtained from the NCBI (National Center for Biotechnology Information) database, including consensus sequences for Zaire ebolavirus (EBOV, n = 172), Sudan ebolavirus (SUDV, n = 20), Bundibugyo ebolavirus (BDBV, n = 8), Taï Forest ebolavirus (TAFV, n = 4), Reston ebolavirus (RESTV, n = 13) and Marburg marburgvirus (MARV, n = 84). In contrast, only one single sequence was available for Lloviu cuevavirus (LLOV).

Statistical analysis. Statistical significance was calculated using unpaired two-tailed t-test employing GraphPad software. Statistical significance is indicated by * = $p < 0.05$, ** = $p < 0.001$, *** = $p < 0.0001$.

288 **RESULTS**

289

290 **The Lloviu virus glycoprotein is a tetherin antagonist.** We employed a previously described
291 HIV Gag-based virus-like particle (VLP) assay (20, 28) to assess inhibition of viral budding by
292 tetherin and its counteraction by EBOV-GP, EBOV-GP mutants and LLOV-GP. HIV Gag was
293 chosen for this endeavor, because expression of filovirus GPs does not modulate release of Gag-
294 VLPs from tetherin-negative cells. In contrast, release of EBOV-VP40-based VLPs from
295 tetherin-negative cells is augmented by EBOV-GP (20), which complicates the analysis of
296 tetherin antagonism. Therefore, a VP40-based assay was only used for confirmatory purposes.
297 We commenced our analysis by asking whether LLOV-GP counteracts tetherin. As a
298 prerequisite to these studies, we determined LLOV-GP expression and facilitation of viral entry.
299 Analysis of epitope-tagged proteins revealed that LLOV-GP and EBOV-GP were appreciably
300 expressed in transfected 293T cells (Fig. 1A), with EBOV-GP expression being more efficient.
301 Moreover, both proteins mediated host cell entry when incorporated into retroviral vectors (Fig.
302 1B), although EBOV-GP-driven entry was more robust than LLOV-GP-mediated entry, in
303 keeping with published data (35). Thus, under the conditions chosen, LLOV-GP was expressed
304 and functional and could be examined for tetherin counteraction. For this, HIV-1 Vpu and
305 EBOV-GP were employed as positive controls while transfection of cells with empty plasmid
306 served as negative control. Tetherin expression reduced Gag-VLP-release and this effect was
307 counteracted by EBOV-GP and Vpu, as expected, and by LLOV-GP (Fig. 1C-D). This
308 observation adds LLOV-GP to the list of viral tetherin antagonists and, jointly with previous
309 work (19, 20), suggests that filoviruses of all three genera, *Ebola*-, *Marburg*- and *Cuevavirus*, can
310 antagonize tetherin via their GPs. In addition, this finding raises the question which features
311 conserved between filovirus GPs control tetherin antagonism

312

313 **Adequate glycosylation of the Ebola virus glycoprotein is required for tetherin antagonism.**
314 A hallmark of all filovirus glycoproteins is their extensive N-linked glycosylation, raising the
315 question whether N-glycans contribute to tetherin counteraction. We employed 293S GnTI$^-$ cells,
316 in which processing of N-glycans is stalled at the high-mannose stage (30), to examine whether
317 appropriate N-glycosylation is a prerequisite to tetherin counteraction by EBOV-GP. Expression
318 of EBOV-GP in transfected control and GnTI$^-$ cells was comparable (Fig. 2A) and pseudotypes
319 produced in both cell lines were readily able to transduce target cells (Fig. 2B). Moreover,
320 tetherin expression restricted Gag-VLP release from both control and GnTI$^-$ cells, with restriction
321 in GnTI$^-$ cells being less effective (Fig. 2C,D), potentially due to a modest accumulation of
322 tetherin in cytoplasmic compartments of these cells (not shown). Thus, tetherin and GP are
323 expressed in biological active forms in control and GnTI$^-$cells. However, EBOV-GP failed to
324 rescue Gag-VLP release from blockade by tetherin in GnTI$^-$cells, while tetherin counteraction by
325 GP was efficient in control cells and tetherin antagonism by Vpu was comparable in both cell
326 lines (Fig. 2C-D). Similar results were obtained when release of VP40-VLPs was examined (Fig.
327 2E), indicating that adequate processing of N-glycans is a prerequisite to tetherin counteraction
328 by EBOV-GP.

329

330 **An intact receptor-binding domain is required for tetherin counteraction by the Ebola virus**
331 **glycoprotein.** We next investigated whether two conserved elements in the GP1 subunit, the
332 mucin-like domain (MLD) and the RBD, are required for tetherin antagonism. Deletion of the
333 MLD was compatible with robust GP expression (Fig. 3A) and slightly increased and decreased
334 GP-driven entry (Fig. 3B), respectively, in agreement with published data (34, 48, 49). Moreover,
335 the MLD was dispensable for tetherin antagonism (Fig. 3C,D), in keeping with a previous study

(19). In order to determine the role of the RBD in tetherin counteraction, we characterized four point mutations in the RBD, three of which were previously reported to abrogate GP-driven host cell entry (F88A, L111A and L122A) (32) while the fourth one was shown not to impede the entry process (W104A) (50). The three amino acid residues essential for entry are fully conserved between members of the genera *Ebolavirus* and *Cuevavirus* and two out of three are also present in the RBD of marburgviruses (the third one was replaced by as conservative substitution, L111I) (Fig. 4A). All mutants were comparably expressed in transfected 293T cells (Fig. 4B and table 1) and mutants F88A, L111A and L122A indeed failed to mediate efficient entry into target cells while entry driven by mutant W104A was robust (Fig. 4C). Notably, the ability of these mutants to drive host cell entry correlated with their capacity to antagonize tetherin: F88A, L111A and L122A exhibited strongly reduced tetherin antagonism in the Gag-VLP assay while W104A was active (Fig. 4D,E). Similar results were obtained in the VP40-VLP assay: F88A, L11A and L122A were unable to appreciably counteract tetherin while tetherin counteraction by mutant W104A was robust (Fig. 4F). Finally, expression of all mutants augmented release of VP40-VLPs from tetherin-negative control cells (Fig. 4F), suggesting that augmentation of VLP release and tetherin antagonism can be genetically separated. In sum, these results show that an intact RBD is required for tetherin antagonism by EBOV-GP.

Inhibition of NPC1 does not interfere with tetherin antagonism by the Ebola virus glycoprotein. During viral entry, proteolytic processing of GP in endosomes exposes the RBD for subsequent binding to NPC1 (17, 18). A recent study reported evidence for the presence of proteolytically processed GP on the surface of 293T cells transfected to express GP (51). Moreover, low levels of endogenous NPC1 were detected at the plasma membrane of 293 cells (51). These observations suggest that NPC1 might not only be required for EBOV-GP-driven

host cell entry but also for tetherin antagonism. To address this possibility, we employed the compound U18666A, a cationic amphiphile (52). U18666A binds to the sterol sensing domain of U18666A (53), induces cholesterol accumulation in endosomes and blocks EBOV entry (42). The compound robustly inhibited EBOV-GP- but not VSV-G-driven entry (Fig. 5A), as expected. A modest inhibition of VSV-G-dependent entry was observed in the presence of 20 µM U18666A (Fig. 5A) and coincided with modestly reduced cell viability (33% reduction as determined by CellTiter-Glo Luminescent Cell Viability assay (Promega), data not shown), suggesting that this effect was unspecific. Despite efficient blockade of GP-driven entry, U18666A treatment did not interfere with tetherin antagonism by EBOV-GP (Fig. 5B,C), indicating that NPC1 functions required for viral entry are dispensable for GP-mediated tetherin antagonism. Several cationic amphiphiles other than U18666A were also found to raise endosomal cholesterol levels and to block EBOV entry in an NPC1-dependent fashion (42). Therefore, we asked whether two of these compounds, clomifene and terconazole, interfere with tetherin antagonism. Both compounds efficiently reduced viral entry, as expected, but did not inhibit tetherin antagonism by GP (Table 2), confirming that biological properties of NPC1 required for GP-driven cell entry are dispensable for tetherin antagonism.

Mutations in the receptor binding domain of the Ebola virus glycoprotein that inhibit tetherin antagonism do not interfere with tetherin binding. It has been reported that EBOV-GP interacts with tetherin (19). Therefore, we investigated whether mutations in the RBD which inhibit tetherin antagonism also block tetherin binding. For this, we first employed co-immunoprecipitation. Expression of EBOV-GP wt, EBOV-GP mutants and tetherin was readily detectable in cotransfected cells and pull-down of tetherin resulted in co-precipitation of wt EBOV-GP (Fig. 6A), as excepted. Notably, wt EBOV-GP and GP mutants with exchanges in the

RBD that inhibit tetherin antagonism were co-precipitated with comparable efficiency (Fig. 6A), suggesting that lack of tetherin antagonism by the RBD mutants tested was not due to lack of tetherin binding. We next investigated whether differences in tetherin binding of EBOV-GP wt and RBD mutants become apparent when endogenous tetherin expression are examined. For this, we transfected HeLa cells, which constitutively express high levels of endogenous tetherin, with plasmids encoding EBOV-GP wt and mutants and determined interactions with tetherin via a proximity ligation assay. We observed comparable tetherin binding of wt and mutant GPs (Fig. 6B,C), confirming that lack of tetherin antagonism by the RBD mutants is not due to lack of tetherin binding.

Evidence that an antibody directed against the GP1 subunit can block tetherin counteraction by the Ebola virus glycoprotein. The results obtained so far pointed towards an important role of the GP1 subunit in tetherin counteraction by EBOV-GP. GP1 is a central target for the humoral immune response and we thus examined whether antibodies directed against GP1 might block tetherin antagonism. For this, we made use of previously described monoclonal antibodies which bind to the MLD in naïve GP and protect mice and guinea pigs from a lethal challenge with EBOV (38, 39). We first assessed whether these antibodies interfere with VLP release from control cells. Antibodies 4G7 and 5D2 did not impact VLP release while antibody 5E6 modestly and antibodies 7G4 and 7C9 strongly inhibited particle release (Fig. 7A,B). Blockade of release might be due to cross-linking of GP on the cell surface and GP on the virion surface, resulting a in a tetherin-like restriction of particle release. When the antibodies were tested on cells coexpressing tetherin and GP, similar results were obtained, with the exception of antibody 5E6 (Fig. 7C,D). This antibody had a modest impact on VLP release from tetherin-negative cells (Fig. 7A,B) but reduced particle release from tetherin-positive cells close to

408 background level (Fig. 7D, dotted line), indicating that it interferes with GP-mediated tetherin
409 antagonism. Finally, it is noteworthy that none of the antibodies inhibited VLP release from
410 tetherin-positive or tetherin-negative cells expressing GP without MLD (not shown), indicating
411 that the above described effects were specific. In sum, our findings suggest that antibody 5E6 can
412 interfere with tetherin antagonism by GP, although part of its release-restricting activity is
413 tetherin-independent.
414
415
416
417
418
419
420
421
422
423
424
425
426
427
428
429
430
431

DISCUSSION

Tetherin is expressed in macrophages (25, 26) and matured dendritic cells (54), which are important filovirus targets (24, 55, 56), and tetherin counteraction by GP might be essential for robust viral spread in the host. However, it is largely unclear how GP antagonizes tetherin and which domains in GP are required. The present study shows that an intact RBD as well as appropriate N-glycosylation of GP are essential for tetherin antagonism and confirms that MLD is dispensable. Moreover, we demonstrate that an antibody against GP1, which protects against fatal EBOV challenge in a mouse model (38), can block tetherin antagonism by GP. These results demonstrate that the GP1 subunit plays a central role in tetherin antagonism and suggest that blockade of GP-dependent tetherin antagonism might contribute to the protective activity of certain anti-GP1 antibodies.

Previous work demonstrated that EBOV-GP (19) and the GPs of other members of the *Ebolavirus* and *Marburgvirus* genera counteract tetherin (20, 28), although these analyses were semi-quantitative and subtle differences in the efficiency of tetherin counteraction might have been missed. In contrast, it was unknown whether the GP of LLOV, which was detected in dead Schreiber's bats (*Miniopterus schreibersii*) in Northern Spain (27), also counteracts tetherin. Absence of tetherin counteraction by LLOV-GP would suggest that LLOV might not be able to spread efficiently in the human host and that LLOV-GP could potentially be used as a tool for mutagenic analysis designed to identify domains required for tetherin antagonism. However, the findings of the present study indicate that LLOV-GP robustly counteracts tetherin, suggesting that tetherin antagonism is conserved between all filoviruses known to date. This finding raises the question which determinants in filovirus GPs are required for tetherin antagonism.

A conserved feature of all filovirus GPs is their extensive N- and O-linked glycosylation. Several N-glycans are located in a surface exposed area, the glycan cap (57), while the mucin-

like domain is extensively modified with O-linked and N-linked glycans. N-glycans limit access to the RBD and are required for binding to cellular lectins and for protection against antibodies (58, 59), since glycans can shield underlying epitopes from binding of neutralizing antibodies. N-glycosylation of proteins starts in the endoplasmic reticulum (ER), where precursor glycans consisting mainly of mannose residues are transferred *en bloc* onto certain asparagine residues. Upon glycoprotein import into the Golgi apparatus, these high-mannose-type N-glycans are processed into hybrid and complex forms. Processing of N-glycans in the Golgi apparatus can be blocked by inactivating GnTI and results in the trapping of N-glycans in their high-mannose from. The present study shows that exclusive modification of GP with high-mannose N-glycans is compatible with efficient GP expression and GP-driven host cell entry, as expected from a previous analysis (60), but may be incompatible with efficient tetherin antagonism. Such a scenario would be in keeping with a recent study reporting that the glycan cap is essential for tetherin antagonism (29), a finding that was confirmed by the present analysis (not shown). However, it cannot be excluded that the absence of tetherin antagonism by GP in GnTI$^-$ cells is due to altered N-glycosylation of tetherin or a cellular factor involved in tetherin antagonism (see discussion below) rather than inappropriate glycosylation of GP itself.

Another hallmark of filovirus GPs, apart from their extensive glycosylation, is the presence of a RBD, which binds to host cell factors involved in viral entry (50, 61, 62). Our study shows that mutations in the RBD which abrogate viral entry also inhibit tetherin antagonism. In contrast, an RBD mutation, which did not interfere with viral entry, was compatible with tetherin antagonism. A straightforward interpretation of these findings is that GP might need to engage the same cellular factor for entry and tetherin counteraction. The cholesterol transporter NPC1 has been identified as a receptor for filoviruses, which is bound by the RBD and which is essential for entry into cultured cells and for viral spread in the host (17, 18, 42, 63). GP binds to

480 NPC1 upon viral uptake into host cell endosomes and processing of GP by the endosomal
481 cysteine proteases cathepsin B and L (17, 18). It is thus not obvious how NPC1 could contribute
482 to tetherin antagonism by GP, which probably occurs at the cell surface or during transport of
483 tetherin to the cell surface. However, a recent study provided evidence that newly expressed GP
484 can be proteolytically processed and transported to the cell surface (51). Moreover, small
485 amounts of NPC1 were detected at the plasma membrane (51). As a consequence, one can
486 speculate that both GP-driven viral entry and tetherin antagonism might depend on NPC1.
487 However, inhibition studies with U18666A and related cationic amphiphiles that induce
488 cholesterol accumulation in endosomes (all compounds) (42), bind NPC1 (U18666A) (53) and
489 block EBOV-GP-driven entry in an NPC1-dependent fashion (all compounds) (42), revealed that
490 blockade of NPC1 functions required for viral entry does not interfere with tetherin antagonism.
491 Notably, the RBD has initially been identified as an element in GP1 which is required for
492 efficient binding of soluble GP1 to the surface of susceptible cells (62), a process believed to be
493 independent of NPC1, due to its predominantly endosomal localization. Subsequent studies
494 provided evidence that cell adherence and susceptibility to GP-driven entry correlate and that
495 adherent (and thus susceptible) cells express an RBD binding partner at the cell surface which is
496 only present in intracellular pools within non-adherent (and thus non-susceptible) cells (64, 65).
497 Although the nature of this cellular factor is at present unknown, it is tempting to speculate that it
498 might not only be required for viral entry but also for tetherin antagonism.

499 Wild type tetherin and artificial tetherin, which was designed in silico, exhibit the same
500 domain organization and exert antiviral activity but share no sequence homology (8). Previous
501 studies reported that EBOV-GP antagonizes the antiviral activity of both proteins (21) and
502 interacts with wt tetherin (19). One can speculate that EBOV-GP may not bind to artificial
503 tetherin, which would suggest that interactions of GP with tetherin might not be required for

tetherin antagonism. Alternatively, GP might bind wt and artificial tetherin and these interactions might be necessary but not sufficient for tetherin counteraction. Both scenarios are in agreement with our finding that RBD mutants largely defective in tetherin counteraction still bind to transfected and endogenously expressed tetherin, as determined by co-immunoprecipitation and proximity ligation assay.

The GP1 subunit is an important target for the antibody response and it is conceivable that antibody binding blocks GP-dependent tetherin antagonism. Indeed, we obtained evidence that one out of five GP1-directed antibodies, which were previously shown to protect mice from lethal EBOV infection (38, 39), may inhibit tetherin antagonism by EBOV-GP, suggesting that this process occurs at the cell surface. However, the analysis and interpretation of this activity is complicated by the observation that this antibody (and two others) also interfere with VLP release from tetherin-negative, GP-expressing cells. The release of Gag-based VLPs is not modulated by GP; the finding that antibodies directed against GP can block this process was therefore unexpected. One explanation could be that these antibodies simultaneously bind to GP on the particle and on the cell surface, resulting in a tetherin-like restriction of particle release. Moreover, the antibody potentially interfering with tetherin antagonism recognizes an epitope in the MLD, a domain that is dispensable for tetherin antagonism. Thus, one must postulate that its interference with tetherin antagonism is not due to the inhibition of MLD interactions with potential cellular binding partners. Instead, the antibody might inhibit conformational changes in GP, which could be required for tetherin counteraction, or might limit the accessibility of epitopes located close to the MLD, due to steric effects. Alternatively, the antibody might reduce GP stability, as has recently been reported for an inhibitor targeting a cavity between GP1 and GP2 (66). In sum, our data suggest that antibodies generated against EBOV-GP1 may interfere

with tetherin antagonism and/or inhibit particle release from tetherin-negative cells in a GP-dependent manner.

Collectively, our study demonstrates a central role of the GP1 subunit, in particular the RBD, in tetherin counteraction and identifies a GP1-specific antibody that may block this process. It will be interesting to investigate whether GP1-specific antibodies generated in EVD patients block tetherin antagonism and whether a previously reported (62, 64, 65) , but so far unidentified cellular interaction partner of the RBD contributes to tetherin antagonism.

ACKNOWLEDGEMENTS

We thank C. Basler, Department of Microbiology, Mount Sinai School of Medicine for the kind gift of plasmids encoding EBOV-GP RBD-mutants. The following reagents were obtained through the NIH AIDS Reagent Program, Division of AIDS, NIAID, NIH: Anti-HIV-1 p24 Monoclonal (71-31) from Dr. Susan Zolla-Pazner and p96ZM651gag-opt from Drs. Yingying Li, Feng Gao, and Beatrice H. Hahn.

REFERENCES

1. **WHO Ebola Response Team.** 2016. Ebola Virus Disease among Male and Female Persons in West Africa. N. Engl. J. Med. **374**:96-98.

2. **WHO.** Ebola Situation Report - 30 December 2015. http://apps.who.int/ebola/current-situation/ebola-situation-report-17-february-2016

3. **Basler, C. F.** 2015. Innate immune evasion by filoviruses. Virology **479-480**:122-130.

4. **Misasi, J. and N. J. Sullivan**. 2014. Camouflage and misdirection: the full-on assault of ebola virus disease. Cell **159**:477-486.

5. **Schoggins, J. W., S. J. Wilson, M. Panis, M. Y. Murphy, C. T. Jones, P. Bieniasz, and C. M. Rice**. 2011. A diverse range of gene products are effectors of the type I interferon antiviral response. Nature **472**:481-485.

6. **Neil, S. J., T. Zang, and P. D. Bieniasz**. 2008. Tetherin inhibits retrovirus release and is antagonized by HIV-1 Vpu. Nature **451**:425-430.

7. **Van Damme N., D. Goff, C. Katsura, R. L. Jorgenson, R. Mitchell, M. C. Johnson, E. B. Stephens, and J. Guatelli**. 2008. The interferon-induced protein BST-2 restricts HIV-1 release and is downregulated from the cell surface by the viral Vpu protein. Cell Host. Microbe **3**:245-252.

8. **Perez-Caballero, D., T. Zang, A. Ebrahimi, M. W. McNatt, D. A. Gregory, M. C. Johnson, and P. D. Bieniasz**. 2009. Tetherin inhibits HIV-1 release by directly tethering virions to cells. Cell **139**:499-511.

9. **Neil, S. J.** 2013. The antiviral activities of tetherin. Curr. Top. Microbiol. Immunol. **371**:67-104.

10. **McNatt, M. W., T. Zang, and P. D. Bieniasz**. 2013. Vpu binds directly to tetherin and displaces it from nascent virions. PLoS. Pathog. **9**:e1003299.

11. **Iwabu, Y., H. Fujita, M. Kinomoto, K. Kaneko, Y. Ishizaka, Y. Tanaka, T. Sata, and K. Tokunaga**. 2009. HIV-1 accessory protein Vpu internalizes cell-surface BST-2/tetherin through transmembrane interactions leading to lysosomes. J. Biol. Chem. **284**:35060-35072.

12. **Vigan, R. and S. J. Neil**. 2010. Determinants of tetherin antagonism in the transmembrane domain of the human immunodeficiency virus type 1 Vpu protein. J. Virol. **84**:12958-12970.

13. **Banning, C., J. Votteler, D. Hoffmann, H. Koppensteiner, M. Warmer, R. Reimer, F. Kirchhoff, U. Schubert, J. Hauber, and M. Schindler**. 2010. A flow cytometry-based FRET assay to identify and analyse protein-protein interactions in living cells. PLoS. One. **5**:e9344.

14. **Douglas, J. L., K. Viswanathan, M. N. McCarroll, J. K. Gustin, K. Fruh, and A. V. Moses**. 2009. Vpu directs the degradation of the human immunodeficiency virus restriction factor BST-2/Tetherin via a {beta}TrCP-dependent mechanism. J. Virol. **83**:7931-7947.

15. **Mangeat, B., G. Gers-Huber, M. Lehmann, M. Zufferey, J. Luban, and V. Piguet**. 2009. HIV-1 Vpu neutralizes the antiviral factor Tetherin/BST-2 by binding it and directing its beta-TrCP2-dependent degradation. PLoS. Pathog. **5**:e1000574.

16. **Mitchell, R. S., C. Katsura, M. A. Skasko, K. Fitzpatrick, D. Lau, A. Ruiz, E. B. Stephens, F. Margottin-Goguet, R. Benarous, and J. C. Guatelli**. 2009. Vpu antagonizes BST-2-mediated restriction of HIV-1 release via beta-TrCP and endo-lysosomal trafficking. PLoS. Pathog. **5**:e1000450.

17. **Carette, J. E., M. Raaben, A. C. Wong, A. S. Herbert, G. Obernosterer, N. Mulherkar, A. I. Kuehne, P. J. Kranzusch, A. M. Griffin, G. Ruthel, C. P. Dal, J. M. Dye, S. P. Whelan, K. Chandran, and T. R. Brummelkamp**. 2011. Ebola virus entry requires the cholesterol transporter Niemann-Pick C1. Nature **477**:340-343.

18. **Cote, M., J. Misasi, T. Ren, A. Bruchez, K. Lee, C. M. Filone, L. Hensley, Q. Li, D. Ory, K. Chandran, and J. Cunningham**. 2011. Small molecule inhibitors reveal Niemann-Pick C1 is essential for Ebola virus infection. Nature **477**:344-348.

19. **Kaletsky, R. L., J. R. Francica, C. Agrawal-Gamse, and P. Bates**. 2009. Tetherin-mediated restriction of filovirus budding is antagonized by the Ebola glycoprotein. Proc. Natl. Acad. Sci. U. S. A **106**:2886-2891.

20. **Kühl, A., C. Banning, A. Marzi, J. Votteler, I. Steffen, S. Bertram, I. Glowacka, A. Konrad, M. Sturzl, J. T. Guo, U. Schubert, H. Feldmann, G. Behrens, M. Schindler, and S. Pohlmann**. 2011. The Ebola virus glycoprotein and HIV-1 Vpu employ different strategies to counteract the antiviral factor tetherin. J. Infect. Dis. **204 Suppl 3**:S850-S860.

21. **Lopez, L. A., S. J. Yang, H. Hauser, C. M. Exline, K. G. Haworth, J. Oldenburg, and P. M. Cannon**. 2010. Ebola virus glycoprotein counteracts BST-2/Tetherin restriction in a sequence-independent manner that does not require tetherin surface removal. J. Virol. **84**:7243-7255.

22. **Lopez, L. A., S. J. Yang, C. M. Exline, S. Rengarajan, K. G. Haworth, and P. M. Cannon**. 2012. Anti-tetherin activities of HIV-1 Vpu and Ebola virus glycoprotein do not involve removal of tetherin from lipid rafts. J. Virol. **86**:5467-5480.

23. **Gustin, J. K., Y. Bai, A. V. Moses, and J. L. Douglas**. 2015. Ebola Virus Glycoprotein Promotes Enhanced Viral Egress by Preventing Ebola VP40 From Associating With the Host Restriction Factor BST2/Tetherin. J. Infect. Dis. **212 Suppl 2**:S181-S190.

24. **Martinez, O., L. W. Leung, and C. F. Basler**. 2012. The role of antigen-presenting cells in filoviral hemorrhagic fever: gaps in current knowledge. Antiviral Res. **93**:416-428.

25. **Schindler, M., D. Rajan, C. Banning, P. Wimmer, H. Koppensteiner, A. Iwanski, A. Specht, D. Sauter, T. Dobner, and F. Kirchhoff**. 2010. Vpu serine 52 dependent counteraction of tetherin is required for HIV-1 replication in macrophages, but not in ex vivo human lymphoid tissue. Retrovirology. **7**:1.

26. **Wrensch, F., C. B. Karsten, K. Gnirss, M. Hoffmann, K. Lu, A. Takada, M. Winkler, G. Simmons, and S. Pohlmann**. 2015. Interferon-Induced Transmembrane Protein-Mediated Inhibition of Host Cell Entry of Ebolaviruses. J. Infect. Dis. **212 Suppl 2**:S210-S218.

27. **Negredo, A., G. Palacios, S. Vazquez-Moron, F. Gonzalez, H. Dopazo, F. Molero, J. Juste, J. Quetglas, N. Savji, M. M. de la Cruz, J. E. Herrera, M. Pizarro, S. K. Hutchison, J. E. Echevarria, W. I. Lipkin, and A. Tenorio**. 2011. Discovery of an ebolavirus-like filovirus in europe. PLoS. Pathog. **7**:e1002304.

28. **Gnirss, K., M. Fiedler, A. Kramer-Kuhl, S. Bolduan, E. Mittler, S. Becker, M. Schindler, and S. Pohlmann**. 2014. Analysis of determinants in filovirus glycoproteins required for tetherin antagonism. Viruses. **6**:1654-1671.

29. **Vande Burgt, N. H., R. L. Kaletsky, and P. Bates**. 2015. Requirements within the Ebola Viral Glycoprotein for Tetherin Antagonism. Viruses. **7**:5587-5602.

30. **Reeves, P. J., N. Callewaert, R. Contreras, and H. G. Khorana**. 2002. Structure and function in rhodopsin: high-level expression of rhodopsin with restricted and homogeneous N-glycosylation by a tetracycline-inducible N-acetylglucosaminyltransferase I-negative HEK293S stable mammalian cell line. Proc. Natl. Acad. Sci. U. S. A **99**:13419-13424.

31. **Sauter, D., M. Schindler, A. Specht, W. N. Landford, J. Munch, K. A. Kim, J. Votteler, U. Schubert, F. Bibollet-Ruche, B. F. Keele, J. Takehisa, Y. Ogando, C. Ochsenbauer, J. C. Kappes, A. Ayouba, M. Peeters, G. H. Learn, G. Shaw, P. M. Sharp, P. Bieniasz, B. H. Hahn, T. Hatziioannou, and F. Kirchhoff**. 2009. Tetherin-driven adaptation of Vpu and Nef function and the evolution of pandemic and nonpandemic HIV-1 strains. Cell Host. Microbe **6**:409-421.

32. **Martinez, O., E. Ndungo, L. Tantral, E. H. Miller, L. W. Leung, K. Chandran, and C. F. Basler**. 2013. A mutation in the Ebola virus envelope glycoprotein restricts viral entry in a host species- and cell-type-specific manner. J. Virol. **87**:3324-3334.

33. **Marzi, A., A. Akhavan, G. Simmons, T. Gramberg, H. Hofmann, P. Bates, V. R. Lingappa, and S. Pohlmann**. 2006. The signal peptide of the ebolavirus glycoprotein influences interaction with the cellular lectins DC-SIGN and DC-SIGNR. J. Virol. **80**:6305-6317.

34. **Neumann, G., H. Feldmann, S. Watanabe, I. Lukashevich, and Y. Kawaoka**. 2002. Reverse genetics demonstrates that proteolytic processing of the Ebola virus glycoprotein is not essential for replication in cell culture. J. Virol. **76**:406-410.

35. **Maruyama, J., H. Miyamoto, M. Kajihara, H. Ogawa, K. Maeda, Y. Sakoda, R. Yoshida, and A. Takada**. 2014. Characterization of the envelope glycoprotein of a novel filovirus, lloviu virus. J. Virol. **88**:99-109.

36. **Wrensch, F., M. Winkler, and S. Pohlmann**. 2014. IFITM proteins inhibit entry driven by the MERS-coronavirus spike protein: evidence for cholesterol-independent mechanisms. Viruses. **6**:3683-3698.

37. **Martin-Serrano, J., T. Zang, and P. D. Bieniasz**. 2001. HIV-1 and Ebola virus encode small peptide motifs that recruit Tsg101 to sites of particle assembly to facilitate egress. Nat. Med. **7**:1313-1319.

38. **Qiu, X., J. B. Alimonti, P. L. Melito, L. Fernando, U. Stroher, and S. M. Jones**. 2011. Characterization of Zaire ebolavirus glycoprotein-specific monoclonal antibodies. Clin. Immunol. **141**:218-227.

39. **Qiu, X., L. Fernando, P. L. Melito, J. Audet, H. Feldmann, G. Kobinger, J. B. Alimonti, and S. M. Jones**. 2012. Ebola GP-specific monoclonal antibodies protect mice and guinea pigs from lethal Ebola virus infection. PLoS. Negl. Trop. Dis. **6**:e1575.

40. **Gorny, M. K., V. Gianakakos, S. Sharpe, and S. Zolla-Pazner**. 1989. Generation of human monoclonal antibodies to human immunodeficiency virus. Proc. Natl. Acad. Sci. U. S. A **86**:1624-1628.

41. **Marzi, A., A. Wegele, and S. Pohlmann**. 2006. Modulation of virion incorporation of Ebolavirus glycoprotein: effects on attachment, cellular entry and neutralization. Virology **352**:345-356.

42. **Shoemaker, C. J., K. L. Schornberg, S. E. Delos, C. Scully, H. Pajouhesh, G. G. Olinger, L. M. Johansen, and J. M. White**. 2013. Multiple cationic amphiphiles induce a Niemann-Pick C phenotype and inhibit Ebola virus entry and infection. PLoS. One. **8**:e56265.

43. **Hoffmann, M., H. M. Gonzalez, E. Berger, A. Marzi, and S. Pohlmann**. 2016. The Glycoproteins of All Filovirus Species Use the Same Host Factors for Entry into Bat and Human Cells but Entry Efficiency Is Species Dependent. PLoS. One. **11**:e0149651.

44. **Berger, R. M. and G. Zimmer**. 2011. A vesicular stomatitis virus replicon-based bioassay for the rapid and sensitive determination of multi-species type I interferon. PLoS. One. **6**:e25858.

45. **Hoffmann, M., M. A. Muller, J. F. Drexler, J. Glende, M. Erdt, T. Gutzkow, C. Losemann, T. Binger, H. Deng, C. Schwegmann-Wessels, K. H. Esser, C. Drosten, and G. Herrler**. 2013. Differential sensitivity of bat cells to infection by enveloped RNA viruses: coronaviruses, paramyxoviruses, filoviruses, and influenza viruses. PLoS. One. **8**:e72942.

46. **Schneider, C. A., W. S. Rasband, and K. W. Eliceiri**. 2012. NIH Image to ImageJ: 25 years of image analysis. Nat. Methods **9**:671-675.

47. **Hagen, N., K. Bayer, K. Rosch, and M. Schindler**. 2014. The intraviral protein interaction network of hepatitis C virus. Mol. Cell Proteomics. **13**:1676-1689.

48. **Medina, M. F., G. P. Kobinger, J. Rux, M. Gasmi, D. J. Looney, P. Bates, and J. M. Wilson**. 2003. Lentiviral vectors pseudotyped with minimal filovirus envelopes increased gene transfer in murine lung. Mol. Ther. **8**:777-789.

49. **Neumann, G., T. W. Geisbert, H. Ebihara, J. B. Geisbert, K. M. Daddario-DiCaprio, H. Feldmann, and Y. Kawaoka**. 2007. Proteolytic processing of the Ebola virus glycoprotein is not critical for Ebola virus replication in nonhuman primates. J. Virol. **81**:2995-2998.

50. **Manicassamy, B., J. Wang, H. Jiang, and L. Rong**. 2005. Comprehensive analysis of ebola virus GP1 in viral entry. J. Virol. **79**:4793-4805.

51. **Markosyan, R. M., C. Miao, Y. M. Zheng, G. B. Melikyan, S. L. Liu, and F. S. Cohen**. 2016. Induction of Cell-Cell Fusion by Ebola Virus Glycoprotein: Low pH Is Not a Trigger. PLoS. Pathog. **12**:e1005373.

52. **Cenedella, R. J.** 2009. Cholesterol synthesis inhibitor U18666A and the role of sterol metabolism and trafficking in numerous pathophysiological processes. Lipids **44**:477-487.

53. **Lu, F., Q. Liang, L. Abi-Mosleh, A. Das, J. K. De Brabander, J. L. Goldstein, and M. S. Brown**. 2015. Identification of NPC1 as the target of U18666A, an inhibitor of lysosomal cholesterol export and Ebola infection. Elife. **4**.

54. **Coleman, C. M., P. Spearman, and L. Wu**. 2011. Tetherin does not significantly restrict dendritic cell-mediated HIV-1 transmission and its expression is upregulated by newly synthesized HIV-1 Nef. Retrovirology. **8**:26.

55. **Geisbert, T. W., L. E. Hensley, T. Larsen, H. A. Young, D. S. Reed, J. B. Geisbert, D. P. Scott, E. Kagan, P. B. Jahrling, and K. J. Davis**. 2003. Pathogenesis of Ebola hemorrhagic fever in cynomolgus macaques: evidence that dendritic cells are early and sustained targets of infection. Am. J. Pathol. **163**:2347-2370.

56. **Ryabchikova, E. I., L. V. Kolesnikova, and S. V. Luchko**. 1999. An analysis of features of pathogenesis in two animal models of Ebola virus infection. J. Infect. Dis. **179 Suppl 1**:S199-S202.

57. **Lee, J. E., M. L. Fusco, A. J. Hessell, W. B. Oswald, D. R. Burton, and E. O. Saphire**. 2008. Structure of the Ebola virus glycoprotein bound to an antibody from a human survivor. Nature **454**:177-182.

58. **Jeffers, S. A., D. A. Sanders, and A. Sanchez**. 2002. Covalent modifications of the ebola virus glycoprotein. J. Virol. **76**:12463-12472.

59. **Lennemann, N. J., B. A. Rhein, E. Ndungo, K. Chandran, X. Qiu, and W. Maury**. 2014. Comprehensive functional analysis of N-linked glycans on Ebola virus GP1. MBio. **5**:e00862-13.

60. **Lin, G., G. Simmons, S. Pohlmann, F. Baribaud, H. Ni, G. J. Leslie, B. S. Haggarty, P. Bates, D. Weissman, J. A. Hoxie, and R. W. Doms**. 2003. Differential N-linked glycosylation of human immunodeficiency virus and Ebola virus envelope glycoproteins modulates interactions with DC-SIGN and DC-SIGNR. J. Virol. **77**:1337-1346.

61. **Brindley, M. A., L. Hughes, A. Ruiz, P. B. McCray, Jr., A. Sanchez, D. A. Sanders, and W. Maury**. 2007. Ebola virus glycoprotein 1: identification of residues important for binding and postbinding events. J. Virol. **81**:7702-7709.

62. **Kuhn, J. H., S. R. Radoshitzky, A. C. Guth, K. L. Warfield, W. Li, M. J. Vincent, J. S. Towner, S. T. Nichol, S. Bavari, H. Choe, M. J. Aman, and M. Farzan**. 2006. Conserved receptor-binding domains of Lake Victoria marburgvirus and Zaire ebolavirus bind a common receptor. J. Biol. Chem. **281**:15951-15958.

63. **Wang, H., Y. Shi, J. Song, J. Qi, G. Lu, J. Yan, and G. F. Gao**. 2016. Ebola Viral Glycoprotein Bound to Its Endosomal Receptor Niemann-Pick C1. Cell **164**:258-268.

64. **Dube, D., K. L. Schornberg, T. S. Stantchev, M. I. Bonaparte, S. E. Delos, A. H. Bouton, C. C. Broder, and J. M. White**. 2008. Cell adhesion promotes Ebola virus envelope glycoprotein-mediated binding and infection. J. Virol. **82**:7238-7242.

65. **Dube, D., K. L. Schornberg, C. J. Shoemaker, S. E. Delos, T. S. Stantchev, K. A. Clouse, C. C. Broder, and J. M. White**. 2010. Cell adhesion-dependent membrane trafficking of a binding partner for the ebolavirus glycoprotein is a determinant of viral entry. Proc. Natl. Acad. Sci. U. S. A **107**:16637-16642.

66. **Zhao, Y., J. Ren, K. Harlos, D. M. Jones, A. Zeltina, T. A. Bowden, S. Padilla-Parra, E. E. Fry, and D. I. Stuart**. 2016. Toremifene interacts with and destabilizes the Ebola virus glycoprotein. Nature **535**:169-172.

795 **FIGURE LEGENDS**

796

797 **FIG 1** The LLOV-GP is a tetherin antagonist. (A) Plasmids encoding V5-tagged versions of the
798 indicated glycoproteins were transiently transfected into 293T cells. Transfection of empty
799 plasmid (Mock) served as negative control. Glycoprotein expression in cell lysates was detected
800 by Western blot analysis, using anti-V5 antibody. Detection of β-actin served as loading control.
801 The results were confirmed in two separate experiments. (B) MLV vectors bearing the indicated
802 glycoproteins were used to transduce 293T cells and luciferase activities in cell lysates was
803 measured at 72 h post transduction. Transduction mediated by EBOV-GP wt was set as 100%.
804 The average ± standard error of the mean (SEM) of five independent experiments is shown. (C)
805 293T cells were transiently transfected with plasmids encoding HIV-Gag, tetherin and the
806 indicated viral glycoproteins or empty plasmid as negative control (Mock). HIV-1 Vpu served as
807 positive control for tetherin antagonism. The presence of Gag in supernatants and cell lysates was
808 determined by Western blot analysis using an anti-Gag antibody. Detection of ß-actin in cell
809 lysates served as loading control. (D) The average of four independent experiments conducted as
810 described for panel C and quantified via the ImageJ program is presented. Release of Gag from
811 cells coexpressing EBOV-GP and tetherin was set to 100%.

812

813 **FIG 2** Processing of N-glycans is required for tetherin antagonism by EBOV-GP but not Vpu.
814 (A) Plasmids encoding the indicated viral glycoproteins were transiently transfected into control
815 293T or GnTI$^-$ cells. Transfection of empty plasmid (Mock) served as negative control.
816 Glycoprotein expression in cell lysates was detected by Western blot analysis, using serum raised
817 against the GP1 subunit of EBOV-GP. Detection of β-actin served as loading control. Three
818 separate experiments yielded similar results. (B) Equal volumes of MLV vectors produced in

819 control or GnTI$^-$ cells and bearing the indicated viral glycoproteins were used to transduce 293T
820 cells. At 72 h post transduction luciferase activities were measured in cell lysates. The results a
821 single representative experiment carried out with triplicate samples are shown. Error bars indicate
822 standard deviation (SD). Similar results were obtained in three separate experiments. C.p.s.,
823 counts per second. (C) GnTI$^-$ cells were transfected with plasmids encoding HIV-Gag, the
824 indicated viral glycoproteins and tetherin or empty plasmid (Mock). HIV-1 Vpu served as
825 positive control for tetherin antagonism. The presence of Gag protein in culture supernatants and
826 cell lysates was determined by Western blot analysis. Detection of ß-actin in cell lysates served
827 as loading control. (D) The average of five independent experiments with control and GnTI$^-$ cells
828 conducted as described for panel C and quantified via the ImageJ program is presented. The
829 release of Gag from cells expressing only Gag without any antagonist and without tetherin was
830 set to 100%, error bars indicate SEM. (E) Control and GnTI$^-$ cells were transfected with plasmids
831 encoding VP40 harboring a myc tag, the indicated viral glycoproteins and tetherin or empty
832 plasmid (Mock). HIV-1 Vpu served as positive control for tetherin antagonism. The presence of
833 VP40 in culture supernatants and cell lysates was determined by Western blot analysis using an
834 anti-myc antibody. The results of single blots are shown from which irrelevant lanes were cut out.
835 Detection of ß-actin in cell lysates served as loading control. Similar results were obtained in
836 three separate experiments.
837
838 **FIG 3** The furin cleavage site in EBOV-GP is required for full tetherin antagonism. (A) Plasmids
839 encoding the indicated viral glycoproteins were transiently transfected into 293T cells.
840 Transfection of empty plasmid (Mock) served as negative control. Glycoprotein expression in
841 cell lysates was detected by Western blot using serum raised against the GP1 subunit of EBOV-
842 GP. Detection of β-actin served as loading control. Three separate experiments yielded similar

843 results. (B) Equal volumes of MLV vectors bearing the indicated glycoproteins were used for
844 transduction of 293T target cells. Luciferase activities in cell lysates were measured at 72 h post
845 transduction. Transduction mediated by EBOV-GP wt was set as 100%. The average ± SEM of
846 five independent experiments is shown. (C) 293T cells were transiently transfected with plasmids
847 encoding HIV-Gag, the indicated viral glycoproteins and tetherin or empty plasmid (Mock).
848 HIV-1 Vpu served as positive control for tetherin antagonism. The presence of Gag protein in
849 supernatants and cell lysates was determined by Western blot using an anti-Gag antibody.
850 Detection of β-actin in cell lysates served as loading control. (D) The average of at least five
851 independent experiments conducted as described for panel C and quantified via the ImageJ
852 program is presented. The release of Gag from cells expressing GP and tetherin was set to 100%,
853 error bars indicate SEM.
854
855 **FIG 4** The EBOV-GP requires an intact receptor-binding domain for tetherin antagonism. (A)
856 Amino acid sequence alignment of the portions (residues 85 to 125 in EBOV-GP) of filovirus
857 receptor-binding domains (RBD) that harbor the amino acid residues investigated for tetherin
858 antagonism (green, numbering according to EBOV-GP). (B) Plasmids encoding the indicated
859 viral glycoproteins were transiently transfected into 293T cells. Transfection of empty plasmid
860 (Mock) served as negative control. Glycoprotein expression in cell lysates was detected by
861 Western blot analysis, using serum raised against GP1 of EBOV-GP. Detection of β-actin served
862 as loading control. Four independent experiments yielded highly comparable results. (B) Equal
863 volumes of MLV vectors bearing the indicated viral glycoproteins were used to transduce 293T
864 cells. Luciferase activity in cell lysates was measured at 72 h post transduction. Transduction
865 mediated by EBOV-GP wt was set to 100%. The average ± SEM of five independent
866 experiments is shown. (C) 293T cells were transfected with plasmids encoding HIV-Gag, tetherin

and the indicated viral glycoproteins or empty plasmid (Mock). HIV-1 Vpu served as positive control for tetherin antagonism. The presence of HIV-Gag in culture supernatants and cell lysates was determined by Western blot. Detection of ß-actin served as loading control. (D) The average of at least five independent experiments conducted as described for panel C and quantified via the ImageJ program is presented. The release of Gag from cells coexpressing GP and tetherin was set to 100%, error bars indicate SEM. (E) 293T cells were transiently transfected with plasmids encoding VP40 harboring a myc tag, tetherin and the indicated viral glycoproteins or empty plasmid (Mock). HIV-1 Vpu served as positive control for tetherin antagonism. The presence of VP40 in culture supernatants and cell lysates was determined by Western blot. Detection of β-actin in cell lysates served as loading control.

FIG 5 U18666A does not block tetherin antagonism by the Ebola virus glycoprotein. 293T cells were treated with the indicated concentrations of compound, incubated with equal volumes of VSV pseudotypes bearing VSV-G or EBOV-GP and luciferase activities in cell lysates were determined at 16 h post transduction. The average of two independent experiments performed with triplicate samples is shown; error bars indicate SEM. Transduction in the absence of inhibitor was set as 100%. (B) 293T cells were cotransfected with plasmids encoding HIV-Gag, tetherin and EBOV-GP or empty plasmid (Mock). HIV-1 Vpu served as positive control for tetherin antagonism. At 12 h post transfection, the indicated concentrations of U18666A were added to cultures expressing EBOV-GP. The presence of HIV-Gag in culture supernatants and cell lysates was determined by Western blot. Detection of ß-actin served as loading control. (C) The average of three independent experiments conducted as described for panel B and quantified via the ImageJ program is presented. The release of Gag from untreated, tetherin-negative control cells was set to 100%, error bars indicate SEM.

FIG 6 Mutations in the receptor binding domain of the Ebola virus glycoprotein that interfere with tetherin antagonism are compatible with tetherin binding. (A) 293T cells were cotransfected with plasmids encoding tetherin with N-terminal AU1 tag and EBOV-GP wt or the indicated EBOV-GP mutants. Co-immunoprecipitation was performed with anti-AU1 antibody coupled to agarose beads and proteins in cell lysates and in precipitates were detected by Western blot analysis, employing rabbit serum raised against the GP1 subunit of EBOV-GP and a rabbit monoclonal antibody directed against tetherin. The results of a single representative experiment are shown and were confirmed in a separate experiment. (B,C) HeLa cells were transfected with plasmids encoding EBOV-GP or the indicated EBOV-GP mutants or empty plasmid as a control. For the Proximity Ligation Assay (PLA), the cells were stained with anti-tetherin and anti-EBOV-GP primary antibodies. The images were analyzed by automatically counting the red spots of 20 transfected cells per sample using Volocity software (version 6.3). Representative microscopic images are shown in panel B. The mean values and standard deviations of the relative amount of PLA spots per cell (n=20) are shown in panel C. The PLA spot count measured for cells transfected with EBOV-GP wt was set to 100%.

FIG 7 Evidence that an antibody directed against the GP1 subunit of EBOV-GP can block tetherin counteraction. (A) 293T cells were transiently transfected with plasmids encoding HIV-Gag and EBOV-GP or empty plasmid (Mock). HIV-1 Vpu served as positive control for tetherin antagonism. At 16 h post transfection, the medium was replaced by fresh culture medium supplemented with the indicated antibodies at a final concentration of 20µg/ml or PBS. The presence of Gag in culture supernatants and cell lysates was determined by Western blot analysis. Detection of β-actin served as loading control. (B) The average of two to five independent

experiments conducted as described for panel A and quantified via the ImageJ program is presented. The release of Gag from cells expressing GP and tetherin was set to 100%, error bars indicate SEM. (C) The experiment was conducted as described for panel A but cells coexpressing tetherin were examined. (D) The average of three independent experiments conducted as described for panel A and quantified via the ImageJ program is presented. The release of Gag from cells expressing GP and tetherin was set to 100%, error bars indicate SEM. The dotted line indicates the assay background, which is defined by VLP release from tetherin-positive cells which do not express a tetherin antagonist.

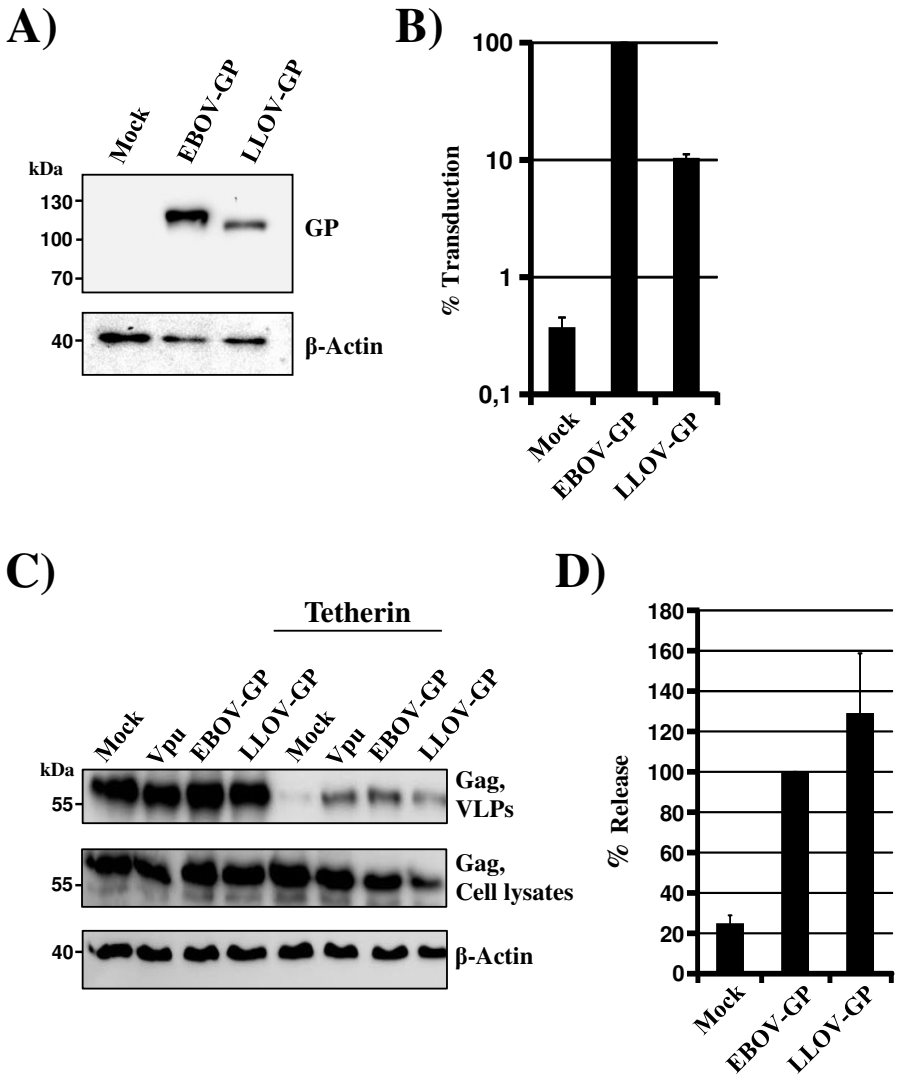

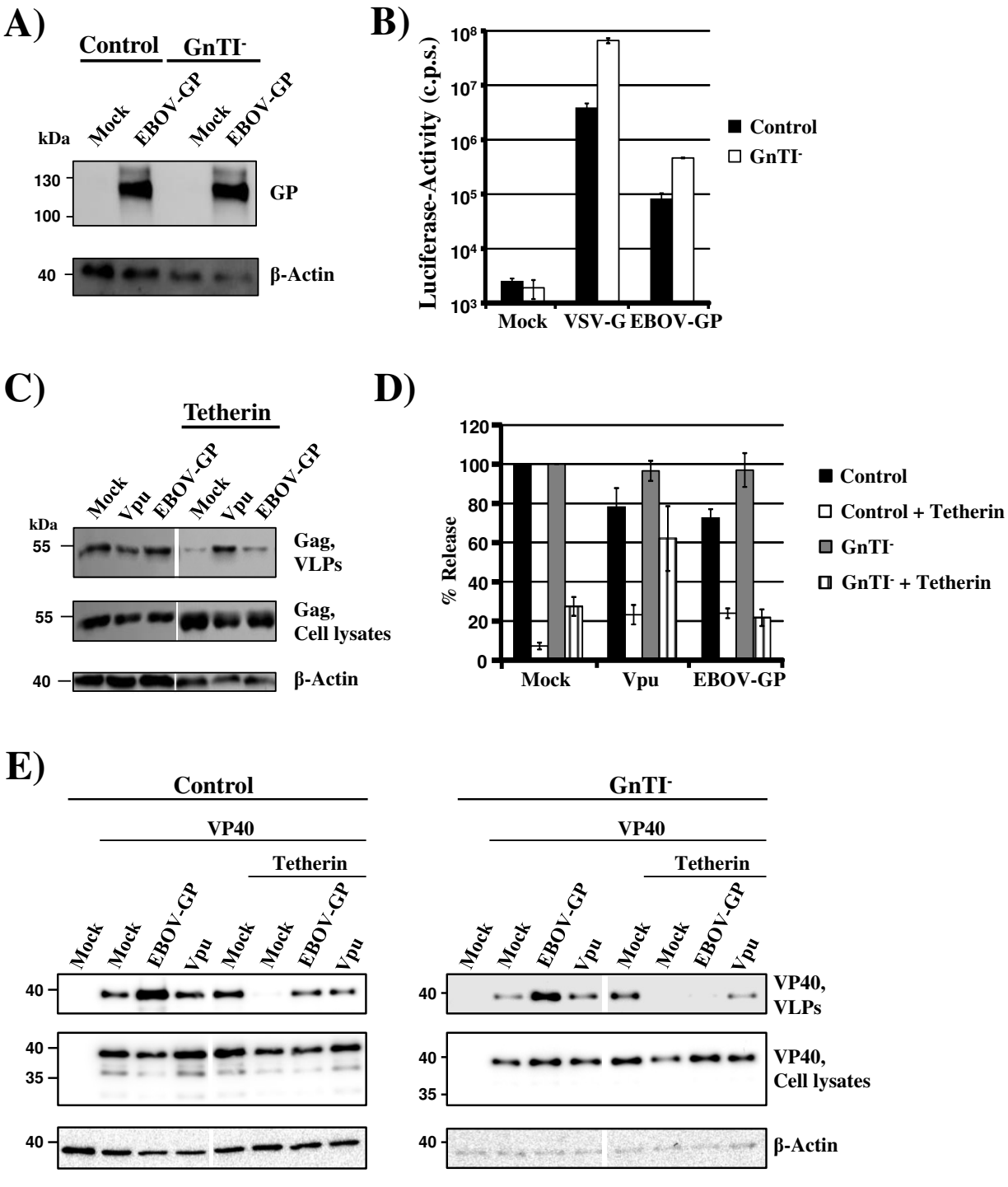

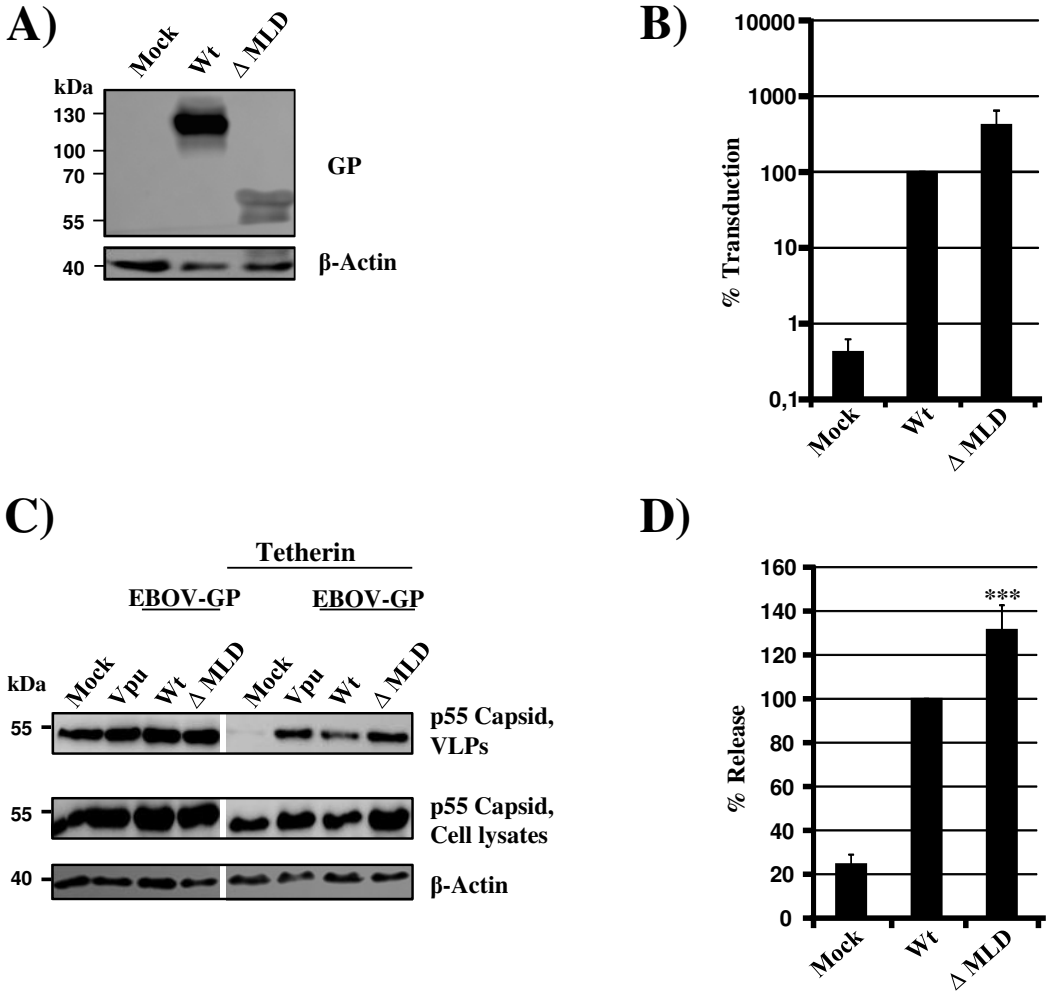

Figure 4

Brinkmann *et al.*

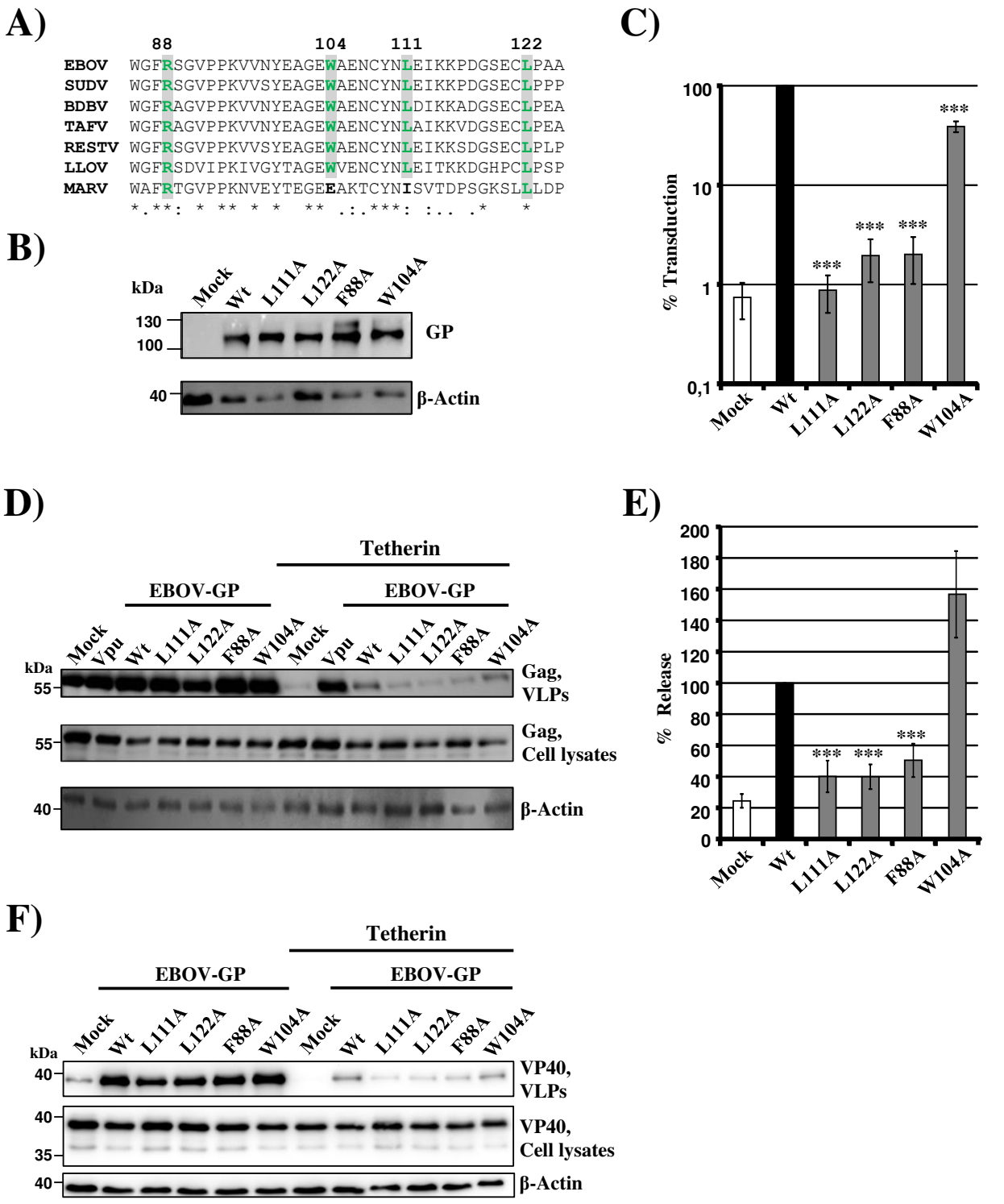

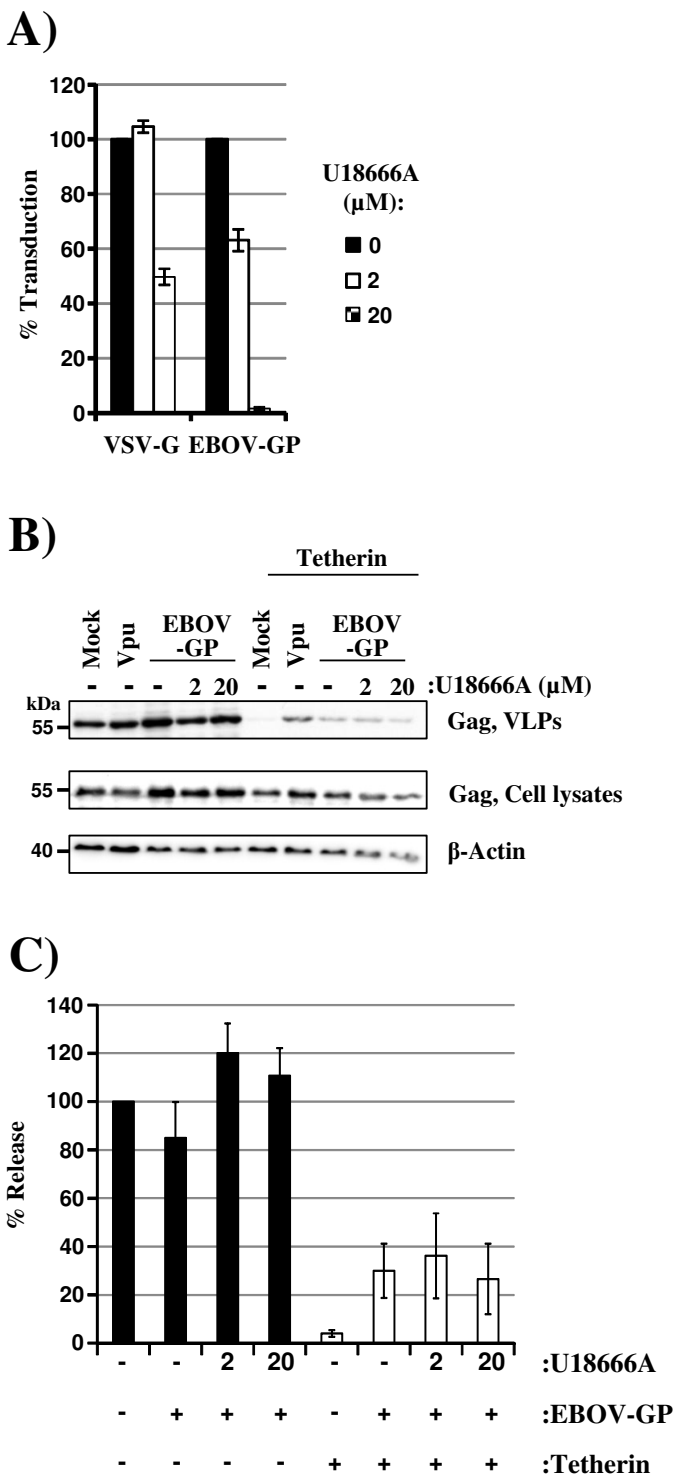

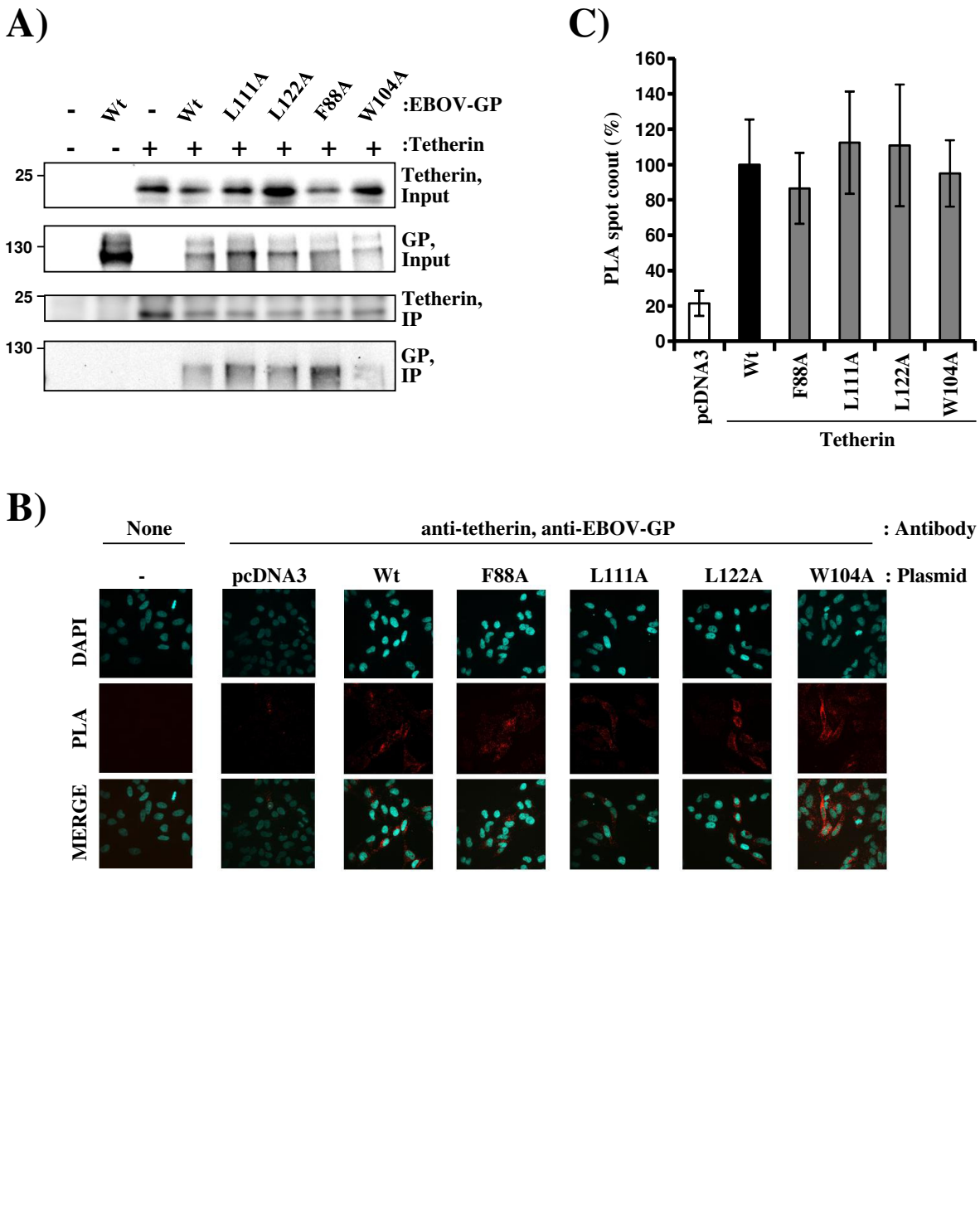

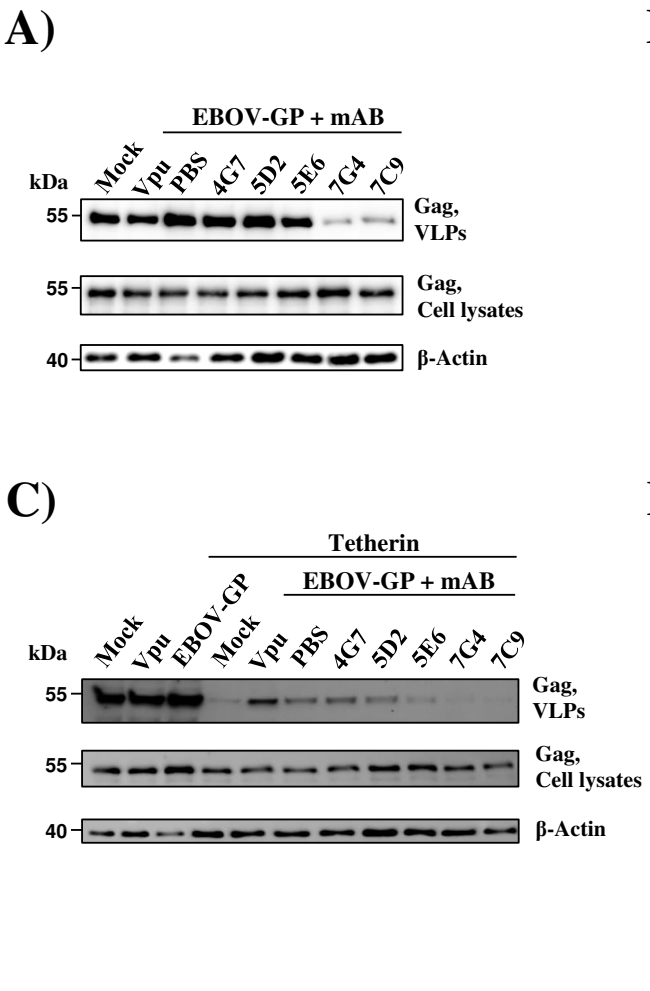

TABLE 1. Expression of the Ebola virus glycoprotein mutants analyzed

Glycoprotein	Expression (%)	
	Cell lysates[a] (Western blot)	Cell surface[b] (FACS)
Wt	100	100
F88A	120.0 ± 10.1	67.7 ± 14.6
L111A	108.6 ± 14.5	45.1 ± 8.4
L122A	120.5 ± 20.5	87.3 ± 12.0
W104A	123.4 ± 15.7	86.7 ± 12.4

[a]Average of three experiments, expression analyzed with rabbit serum raised against GP1

[b]Average of four experiments, expression analyzed with antibody 5E6

TABLE 2. Inhibition of Ebola virus glycoprotein-driven entry and tetherin antagonism by cationic amphiphiles

Inhibitor	Concentration (μM)	Cell Viability[a]	Entry Inhibition[a]	Release Inhibition[a]
Chlomifene	5	++	+++	-
Terconazole	9.4	+++	+++	-
U18666A	20	++	+++	-

[a] +++, ≥75% ; ++, ≥ 50%; +, ≥ 25%; -, < 25%